Construction of a template family for the detection of gravitational waves from coalescing binaries

Theocharis A. Apostolatos

Max–Planck–Society, Research Unit "Theory of Gravitation" at the Friedrich–Schiller–University, D-07743 Jena, Germany

A discrete set of theoretical waveforms should be ready to use when searches for gravitational waves at the noisy output of the laser interferometric detectors that are presently under construction begin. In this paper we extend the method introduced by Sathyaprakash and Dhurandhar to construct such a family of templates, that was based on simple Newtonian signals, to post^2-Newtonian signals that may be modulated due to spin-induced precession. More specifically, we show that if post-Newtonian terms of the phase are taken into account then the Newtonian templates turn out to be a rather inadequate type of search templates and other templates of higher post-Newtonian order should be used instead. This expands the number of parameters that the templates depend on, and, therefore, it leads to a required number of templates that is 2 orders of magnitude larger than it was previously thought, when precessionally modulation effects are ignored and a formidable number of templates when precessionally modulated signals are considered. From our analysis it becomes clear that a post$^{1.5}$-Newtonian family of templates, with vanishing spin term, is a very promising family of search templates for signals coming from nonprecessing binaries. Furthermore, adding an extra oscillatory term in the phase of these post$^{1.5}$-Newtonian templates would extend their detecting ability to signals coming from moderately precessing binaries; but, unfortunately, the number of templates then needed leaves no hope for an on-line search. This extended family of templates could be used more effectively in a hierarchical off-line search. [S0556-2821(96)01714-6]

PACS number(s): 04.80.Nn, 04.30.Nk, 95.30.Sf, 95.75.Pq

I. INTRODUCTION

The first ground-based laser-interferometer gravitational-wave detectors are already under construction and within the first decade of the next millennium a network of at least four such detectors [the two Laser Interferometric Gravitational Wave Observatories (LIGO's), VIRGO, and GEO600] is expected to be able to collect data and search for gravitational waves. The most promising and well-understood sources of gravitational waves are merging compact binaries.

For detecting these gravitational waves, in addition to a highly sophisticated technical design of detectors, a carefully constructed family of theoretical models, called templates, for the signal is needed [1]. Since the corresponding signal is expected to be buried in the detector's noise, only by cross correlating the noisy output of the detector with all members of a pre-constructed family of templates we might have good chances for detecting some gravitational wave from a binary source.

To obtain the highest possible signal-to-noise ratio for some given signal, and thus to increase the probability to detect the corresponding gravitational wave, at least one member of the template family should very accurately mimic the signal. Of course, the task of constructing a family of extremely accurate templates is completely unrealistic since (i) one should first solve the full relativistic two-body problem which is a very difficult, and very complicated problem, that still remains unsolved and (ii) the number of parameters that characterize the signal, though relatively small, would lead to an enormous bank of templates that exceeds by far the near-future computer capabilities. The only way out is to construct approximate signal models based on post-Newtonian techniques, and get rid of all the parameters that do not crucially affect the shape of the signal (e.g., the distance to the source; see Ref. [2]), and those ones that are expected, on theoretical grounds, to have some preferred value (e.g., the eccentricity of the binary's orbit is expected to be nearly zero for almost all binaries under consideration; see [3,4]).

The Newtonian family of templates, that is the family of waveforms based on the quadrupole-moment formalism for two pointlike masses orbiting around each other in circular orbits, has for long been considered a "good" family of search templates for detection purposes and extensive work has been done [5–7] in the past to exhibit its power for detection, its simplicity, and the small number of such templates one needs. The Newtonian waveforms depend only on three parameters: the time to coalescence, the phase at coalescence, and some specific combination of the two masses, called chirp mass. (The rest of the parameters, that are related to the geometry of the binary with respect to the detector, combine to a numerical factor that simply multiplies the waveform function without affecting its shape [2].) Now, the time to coalescence will be taken into account directly in the computing process, while performing the cross correlations via fast Fourier transforms, and for the phase at coalescence only two values are needed (cf. [8,9]). The Newtonian waveforms then depend, in a nontrivial way, only on the chirp mass. Therefore, the problem of constructing a family of Newtonian search templates reduces to the problem of choosing a set of carefully spaced values for the chirp mass that covers the whole range of masses of the potentially detectable binaries.

Only recently, our confidence to the Newtonian family of templates has started shaking. By using the fitting factor (FF)

as a tool to measure the adequateness of a family of templates Apostolatos [9] has demonstrated the highly diminished power of a Newtonian waveform to mimic a signal waveform described by the highest available post-Newtonian approximations within the sensitive frequency range of the advanced LIGO detectors (10 Hz to ~ 200 Hz). Schutz [10] has suggested using the Newtonian family of templates in a narrower window of frequencies where all post-Newtonian effects on the signal are not yet significant. We have tested this and found that, although one may gain a bit in the signal-to-noise ratio, the maximum value of the corresponding FF is still low; this indicates that these *truncated* Newtonian templates are not much better than the plain Newtonian templates.

As it was shown in Ref. [9], a family consisting of at least post$^{1.5}$-Newtonian waveforms is needed to fit better a realistic signal waveform, and thus produce a high cross-correlation output. The problem that arises then is that by using templates of higher and higher post-Newtonian order one introduces more and more parameters (another mass function, besides the chirp mass, shows up in post^1-Newtonian order, some spin parameter shows up for first time in post$^{1.5}$-Newtonian order, and so on), and that may imply a huge number of corresponding templates. Sathyaprakash [11] has shown that with a clever choice of a new version of the chirp mass parameter one could take into account the post-Newtonian effects and still keep the problem one dimensional. Unfortunately, the output of our present work contradicts the results of Sathyaprakash. This contradiction is due to different ranges of frequencies and noise spectra assumed. Our work assumes a realistic colored noise and an upper frequency cutoff set at the frequency of the last stable circular orbit. It turns out from our work that we have to deal with the two-dimensional parameter space of a post$^{1.5}$-Newtonian family of templates (the omission of the spin parameter does not substantially reduce the FF values one obtains, as we had shown in Ref. [9]). This results in an increase in the number of templates needed by almost 2 orders of magnitude as compared with previous estimations based on Newtonian templates.

As was shown by Apostolatos, Cutler, Sussman, and Thorne in Ref. [12], if the orbital angular momentum of the binary and its spins are not aligned, then its orbital plane will precess, leading to modulation on both the amplitude and the phase of its gravitational wave. Apostolatos [9] has demonstrated the difficulties imposed on detecting such signals by using simple post-Newtonian templates, especially when the opening angle of precession is not small. Here, we investigate the effects of precession on the total number of templates needed and suggest the expansion of the templates' parameter space by three more parameters to improve the effectiveness of templates on detecting signals that are moderately modulated. (Highly modulated signals are very complicated; so even these new extended templates are not able to produce sufficiently high FF's.) If these extended templates were to be included in the bank of search templates, one would need a huge number of templates that exceeds by far the present and near-future computer capabilities. Thus, they, or any other kind of templates that may be used to "correct" the precessionally modulated signals, should be used at a second detection stage, off line.

The rest of this paper is organized as follows. In Sec. II we briefly review the definition and physical significance of FF as a useful tool to measure the adequateness of some family of templates. The noise spectral density is assumed to be that of an "advanced detector" [13]. We also present all post-Newtonian approximations for the gravitational waveforms, that are available today, in a compact form that will be helpful in our analysis. In the stationary phase approximation all post-Newtonian waveforms have the same amplitude form, but different phase forms. (Actually, there are post-Newtonian corrections to the amplitude but they turn out to be negligible, compared to the post-Newtonian corrections to the phase; see Ref. [2].) For the waveform describing a true signal we are using the highest post-Newtonian waveform, namely the post^2-Newtonian one [14].

In Sec. III we demonstrate for one more time the fact that both Newtonian and post^1-Newtonian templates are not sufficiently adequate as search templates, by expanding Table I of Ref. [9] so as to include the post^2-Newtonian waveforms; see Table I. The FF values obtained for all possible combinations of signals and templates, for some characteristic binaries, suggest that the post$^{1.5}$-Newtonian templates with vanishing spin term are good enough for detection purposes, even for signal waveforms that are of higher than post^2-Newtonian order. Finally, by truncating the Newtonian templates to some fixed uppermost frequency in order to avoid the template-signal phase mismatching due to post-Newtonian terms in the signal, as Schutz [10] has suggested, we have shown that it is not very effective in improving the performance of the Newtonian templates.

In Sec. IV we analyze the method we have used to cover the whole parameter space (a two-dimensional space) with carefully spaced templates so that any possible signal cross correlated with at least one of the fixed templates produces an output only slightly lower (10% at most) than the output which it would have produced with a hypothetical template that would perfectly mimic the signal. This is an extension in two dimensions of the method used by Sathyaprakash and Dhurandhar [5], but it is far more complicated since the distances between neighboring templates depend greatly on the masses and the spins of the binary, and the parameter space that has to be covered has irregular shape. After discussing the problems arising in counting the number of templates, that one needs to have in a bank of templates, we present a more or less accurate estimation of that number.

In Sec. V we briefly present the numerical process that is expected to be followed at the first stage of detection, and transform our results for the number of templates to computer power requirements.

In Sec. VI we discuss the implications arising from considering signals from spin-induced precessing binaries. After exploring the precessional effects induced in the phase and the amplitude of such a signal, we make an attempt to construct an extended post$^{1.5}$-Newtonian family of templates able to detect these complicated signals and give an order of magnitude estimation of the number of its members.

Finally, in Sec. VII we summarize our results and suggest ways to exploit our results for precessionally modulated signals.

In Appendix A and Appendix B we present semiquantitative arguments for simplifying and modeling the modula-

TABLE I. This table presents the FF values for a Newtonian, a post[1]-Newtonian, a post[1.5]-Newtonian signal with maximal spin parameter β, and a post[2]-Newtonian signal with maximal spin parameters β and σ, being searched for by the four corresponding families of templates: the Newtonian family, the post[1]-Newtonian family, the post[1.5]-Newtonian family with vanishing spins, and the post[2]-Newtonian family with vanishing spins. For every case, two FF values are given, corresponding to a $10M_\odot,1.4M_\odot$ black-hole–Neutron-star (BH/NS) binary and a $1.4M_\odot,1.4M_\odot$ NS-NS binary. The modulational effects are absent since the spins and angular momenta are considered aligned. The numbers quoted in this table are discussed more extensively in Sec. III.

	N signal	P^1-N signal	$P^{1.5}$-N signal (β maximal)	P^2-N signal (β,σ maximal)
N templates:	1.000 (BH-NS) 1.000 (NS-NS)	0.559 (BH-NS) 0.465 (NS-NS)	0.677 (BH-NS) 0.535 (NS-NS)	0.669 (BH-NS) 0.531 (NS-NS)
P^1-N templates:		1.000 (BH-NS) 1.000 (NS-NS)	0.719 (BH-NS) 0.612 (NS-NS)	0.729 (BH-NS) 0.620 (NS-NS)
$P^{1.5}$-N templates: ($\beta=0$)			0.988 (BH-NS) 0.986 (NS-NS)	0.990 (BH-NS) 0.993 (NS-NS)
P^2-N templates: ($\beta,\sigma=0$)				0.979 (BH-NS) 0.989 (NS-NS)

tional effects appearing in the phase of signals that are produced from precessing binaries.

Throughout we assume that all binaries' are circular and we use units where $G=c=1$.

II. THE FF AS A TOOL FOR MEASURING THE ADEQUATENESS OF A TEMPLATE FAMILY

A. Definition and significance of the FF

As was shown in the work of Apostolatos [9], if the family of search templates used at the detection stage does not contain the true signal waveform, then the signal-to-noise ratio will be reduced by

$$\left(\frac{S}{N}\right)=\text{FF}\times\left(\frac{S}{N}\right)_{\text{max}}, \qquad (1a)$$

where

$$\text{FF}=\max_{\lambda_1,\lambda_2,\dots}\frac{(W|T_{\lambda_1,\lambda_2,\dots})}{\sqrt{(T_{\lambda_1,\lambda_2,\dots}|T_{\lambda_1,\lambda_2,\dots})(W|W)}}. \qquad (1b)$$

In Eq. (1) $(S-N)_{\text{max}}$ is the signal-to-noise ratio we would obtain if we had used the exact signal waveform $W(t)$ as a template, and $T_{\lambda_1,\lambda_2,\dots}(t)$ is a member of the template family parametrized by the parameters $\lambda_1,\lambda_2,\dots$. The inner product of two waveforms $(h_1|h_2)$ is defined [2] by

$$(h_1|h_2)=2\int_0^\infty\frac{\widetilde{h}_1^*(f)\widetilde{h}_2(f)+\widetilde{h}_1(f)\widetilde{h}_2^*(f)}{S_n(f)}df, \qquad (2a)$$

where $\widetilde{h}(f)$ represents the Fourier transform of $h(t)$, an asterisk as a superscript denotes complex conjugate, and $S_n(f)$ is the spectral density of the detector's noise which here is assumed to be that of the "advanced LIGO detector" [13], an analytic fit of which has been given in Ref. [2]:

$$S_n(f)=\begin{cases}\infty & \text{for }f<10\text{ Hz},\\ S_0\left[\left(\frac{f_0}{f}\right)^4+2\left(1+\left(\frac{f}{f_0}\right)^2\right)\right] & \text{for }f\geqslant10\text{ Hz},\end{cases} \qquad (2b)$$

where $S_0=0.6\times10^{-48}\text{Hz}^{-1}$ and $f_0=70$ Hz. Of course, the unavoidable fact of the reduced signal-to-noise ratio—partly because of using templates that are not accurately mimicing a realistic signal and partly because of using a discrete family of templates—will lead to a lower threshold setting for detection and thus to a higher false alarm rate.

In this paper we have decided to set the limit of 0.9 as the lowest acceptable FF value for some template family to be considered adequate, since a reduction in signal-to-noise ratio by 10% means a 27% loss in the event rate. On the other hand a 10% reduction in signal-to-noise ratio is equivalent to roughly 10% shortening of the detectors' arms.

B. Review of the post-Newtonian waveforms

An ongoing effort of theorists [14] has already produced analytic expressions for the waveforms of gravitational waves coming from compact binaries up to post[2]-Newtonian order, that is through order $(v/c)^4$ (where v is the orbital velocity) beyond the quadrupole formula. In the stationary phase approximation, and after neglecting all post-Newtonian corrections to the amplitude, the post-Newtonian waveforms can be written in the compact form

$$h_i(f)=\mathcal{A}f^{-7/6}e^{i\psi_i(f)}, \qquad (3a)$$

where $\mathcal{A}$ is a constant depending on the relative geometry of the binary with respect to the detector and on some combination of the masses m_1, m_2 of the binary, and i takes one of the values 0,1,1.5,2 denoting the corresponding post-Newtonian order (post^2-Newtonian order is the higher order included in our analysis); $h_0(f)$ is simply the Newtonian waveform. The phase functions $\psi_i(f)$ of the various post-Newtonian orders are given by [14]

$$\begin{pmatrix} \psi_0(f) \\ \psi_1(f) \\ \psi_{1.5}(f) \\ \psi_2(f) \end{pmatrix} = G(f) + H(f) \begin{pmatrix} 1 & 0 & 0 & 0 \\ 1 & 1 & 0 & 0 \\ 1 & 1 & 1 & 0 \\ 1 & 1 & 1 & 1 \end{pmatrix} \begin{pmatrix} 1 \\ \dfrac{20}{9}\left(\dfrac{743}{336} + \dfrac{11\mu}{4M}\right)(\pi M f)^{2/3} \\ -4(4\pi - \beta)(\pi M f) \\ 10\left(\dfrac{3\,058\,673}{1\,016\,064} + \dfrac{5429\mu}{1008M} + \dfrac{617\mu^2}{144M^2} - \sigma\right)(\pi M f)^{4/3} \end{pmatrix}, \tag{3b}$$

where

$$G(f) = 2\pi f t_C - \phi_C - \pi/4, \tag{3c}$$

and

$$H(f) = \frac{3}{128}(\pi \mathcal{M} f)^{-5/3}. \tag{3d}$$

The three mass parameters $M, \mu, \mathcal{M}$ represent the total mass ($M = m_1 + m_2$), the reduced mass ($\mu = m_1 m_2/M$), and the chirp mass [$\mathcal{M} = (m_1^3 m_2^3/M)^{1/5}$], respectively; t_C and ϕ_C are the time and phase at coalescence, and the two terms β and σ are the so-called spin-orbit and spin-spin terms, respectively, that are given by

$$\beta = \frac{1}{M^2}\left[\left(\frac{113}{12} + \frac{25m_2}{4m_1}\right)\mathbf{S_1} + \left(\frac{113}{12} + \frac{25m_1}{4m_2}\right)\mathbf{S_2}\right]\cdot\hat{\mathbf{L}}, \tag{3e}$$

and

$$\sigma = \frac{1}{48m_1 m_2 M^2}[-247\mathbf{S_1}\cdot\mathbf{S_2} + 721(\mathbf{S_1}\cdot\hat{\mathbf{L}})(\mathbf{S_2}\cdot\hat{\mathbf{L}})], \tag{3f}$$

where $\mathbf{S_1}$ and $\mathbf{S_2}$ are the two bodies' spins, and $\hat{\mathbf{L}}$ is the unit vector along the direction of the binary's orbital angular momentum.

It should be noted here that in the presence of spins the waveform depends on the spins not only through the spin terms β and σ but also through the spin-induced precessional changes in the geometry of the binary that produce a modulation in the amplitude and an extra modulation in the phase of the gravitational waveforms that arrive on Earth (see Ref. [12]). For the moment we will avoid all these complications caused by precession, assuming either that spins are vanishing or that they are aligned with respect to the orbital angular momentum.

C. The form of FF for post-Newtonian waveforms

By specializing to post-Newtonian waveforms both for the signal and for the templates used to detect the signal, FF takes the explicit form

$$\text{FF} = \max_{\Delta t_C, \Delta(\mathcal{M}^{-5/3}), [\Delta(M^{1/3})]} \frac{\left|\int_0^\infty df[f^{-7/3}/S_n(f)]e^{i\Delta\psi(f)}\text{AM}\times\text{PM}\right|}{\sqrt{\left[\int_0^\infty df[f^{-7/3}/S_n(f)]\right]\left[\int_0^\infty df[f^{-7/3}/S_n(f)](\text{AM})^2\right]}}, \tag{4}$$

where AM and PM are some amplitude and phase modulation factors, that are present whenever the spin-induced precession of the binary is turned on; otherwise these modulational terms could be omitted. $\Delta\psi(f)$ is the difference between the signal's phase function and the template's phase function, apart from any precessional modulation, and $\Delta t_C, \Delta(\mathcal{M}^{-5/3}), \Delta(M^{1/3})$ are the differences between the corresponding parameters of the signal and of any member of the chosen template family. Especially $\Delta(M^{1/3})$ is written in square brackets to show that it has to be used *only* if the template family is not the Newtonian one, since the Newton-

ian templates depend on the masses of the binary only through the chirp mass. For templates of higher post-Newtonian order one more mass function, besides the chirp mass, is needed to define the template. Here, we have decided to use the total mass $M^{1/3}$ because it turned out to be easier to handle in our analysis and our numerical code; the results we have obtained do not depend on that choice. One of the parameters of the waveforms, ϕ_C, is not present in Eq. (4) since we have already maximized the expression for FF over this parameter by keeping the absolute value of the numerator in the right-hand side of Eq. (4).

It should be noted that the post-Newtonian order of the signal is assumed to be of greater or equal order than that of the templates, since the signal is supposed to be described by the most accurate available waveform while the templates are usually considered to have a simpler form than the signal. In order to keep the number of templates in the chosen family moderately low we will assume that all templates correspond to waveforms with vanishing spin terms. [This explains why the β and σ terms do not show up in the set of parameters over which the expression in Eq. (4) is maximized.] In the next section we will justify this simplification by demonstrating in what extent this is harmless for detection purposes.

III. THE INADEQUATENESS OF THE NEWTONIAN TEMPLATE FAMILY

In this section we present once more the results obtained by Apostolatos [9] for the FF values one gets if various post-Newtonian template families and various nonmodulational post-Newtonian signals are used, augmented by some additional results that we obtained by incorporating the recently discovered nonmodulational post^2-Newtonian effects [14]. More specifically, in Table I we have computed the FF values obtained if any of the Newtonian, post^1-Newtonian, post$^{1.5}$-Newtonian with $\beta = 0$, or post^2-Newtonian with $\beta = \sigma = 0$ template families is used as a family of search templates to detect signals described by any of the post-Newtonian waveforms of Eqs. (3). (One can find similar tables in [6].) As we discussed in the previous section, in order to avoid expanding enormously the parameter space of the template families, all our templates correspond to post-Newtonian waveforms with vanishing spin terms; that is

$$\psi_i^{\text{templ}}(f) = \psi_i(f; S_1 = S_2 = 0). \qquad (5)$$

However, the analogous post-Newtonian signals have been chosen with maximal β and σ terms so as to get an estimation for the FF values in the worst case; that is, when the mismatch between the waveform of the template and that of the signal is maximum. Some slight disagreement in the entries of the $P^{1.5}$-N column between the present Table I and the Table I of [9] is due to the fact that in the present case both objects of the binary are assumed to have spin which are aligned with the binary's orbital angular momentum while in Ref. [9] only the more massive body was spinning.

It is clear from Table I that for search templates of order lower than post$^{1.5}$-Newtonian, the FF values obtained for signal waveforms that are of higher post-Newtonian order than the template family are rather poor. This indicates that the Newtonian and the post^1-Newtonian families of templates are rather inadequate families of search templates. On the other hand, the slightly differing, but quite high, FF values for both the post$^{1.5}$-Newtonian and the post^2-Newtonian templates suggest that the post$^{1.5}$-Newtonian family of templates might be quite adequate for detection purposes. The inclusion of the post^2-Newtonian term in the signal changes very slightly the fitting capability of the post$^{1.5}$-Newtonian family of templates. (It actually produces a FF value a bit higher than the FF for a post$^{1.5}$-Newtonian signal.) This is an indication that inclusion of further post-Newtonian terms in the signal might not produce significantly lower FF values. For a post^2-Newtonian signal, the post^2-Newtonian family of templates does produce lower FF than the post$^{1.5}$-Newtonian one since β and σ in a post^2-Newtonian signal have opposite signs and thereby they tend to cancel each other. Nevertheless, the difference is small and presumably it is even smaller for a family of templates of higher order. All these explain why we have chosen to use the post$^{1.5}$-Newtonian family of templates in our paper.

At this point we should note that the FF values we presented in Table I are based on the assumption of a continuous parameter space for the templates. This is unrealistic since only a finite number of templates can be handled by computers when cross correlating the signal with all the members of some chosen template family. However, this unrealistic assumption was necessary in order to find out what kind of templates are sufficiently ''flexible'' to mimic satisfactorily a true gravitational signal, and produce a FF value well above 0.9. Of course the FF is expected to be further reduced when a discrete set of templates is considered. This will be our subject in the following sections.

The simplicity of the Newtonian templates and moreover their dependence on a small number of parameters has forced people to develop some tricks to increase their detectability. Schutz [10] especially has proposed to truncate the Newtonian templates at some frequency where the post-Newtonian effects start growing large. His argument was that up to this frequency limit a Newtonian template could very accurately match a true signal, while it is not fair to call the Newtonian templates ''inadequate'' on grounds that they perform badly through the whole range of frequencies where the detectors are sensitive.

Hence, we investigated this idea by computing the FF obtained by a truncated Newtonian family as a function of the truncation frequency. To be more specific, we have computed numerically the function

$$\text{FF}(f_{\text{trunc}}) = \max_{\Delta t_C, \Delta(\mathcal{M}^{-5/3})} \frac{\left| \int_0^{f_{\text{trunc}}} df [f^{-7/3}/S_n(f)] e^{i[\psi_i^{\text{sign}}(f) - \psi_0^{\text{templ}}(f)]} \right|}{\sqrt{\left[\int_0^{f_{\text{trunc}}} df [f^{-7/3}/S_n(f)] \right] \left[\int_0^{\infty} df [f^{-7/3}/S_n(f)] \right]}}, \qquad (6)$$
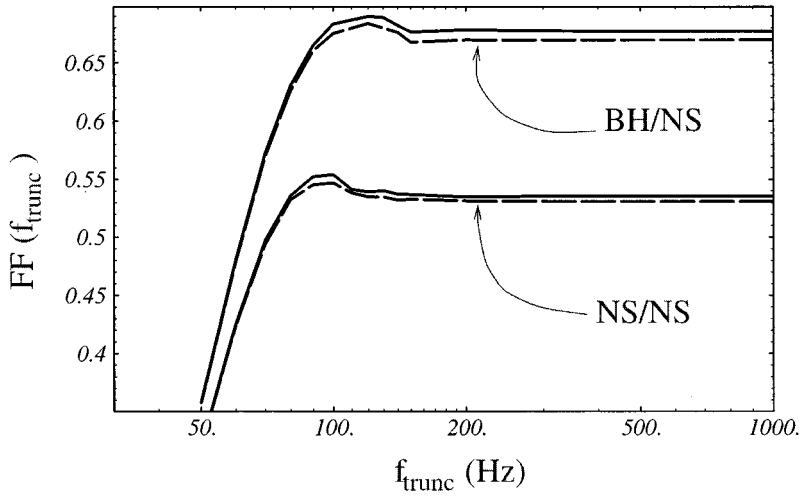
FIG. 1. This plot shows the performance of a truncated Newtonian family of templates on detecting a post$^{1.5}$-Newtonian signal (solid lines), or a post^2-Newtonian signal (dashed lines) as a function of the uppermost frequency f_{trunc} of the templates. The top pair of lines corresponds to a signal from a $10M_\odot, 1.4M_\odot$ BH-NS binary with both bodies maximally rotating ($S_i = m_i^2$), and both spins and orbital angular momentum aligned. The bottom lines correspond to an analogous $1.4M_\odot, 1.4M_\odot$ NS-NS binary. The small hump in all cases indicates a slight, but not satisfactory, improvement on the performance of the truncated templates over the plain ones.

which arises from Eq. (4) if we omit the modulational factors AM and PM and set f_{trunc} as the uppermost frequency present in the Newtonian templates. In Fig. 1, the dependence of $FF(f_{trunc})$ on f_{trunc}, both for a post$^{1.5}$-Newtonian ($i=1.5$) and a post^2-Newtonian signal ($i=2$) from two typical binaries, is depicted. It is clear that although one may gain somewhat higher FF (higher signal-to-noise ratio) by cutting the cross correlation of the Newtonian templates and the signal at some frequency f_{trunc}, this method is not very effective since a significant part of the whole signal is then lost by reducing f_{trunc} to avoid the post-Newtonian behavior of the signal. The maximum possible FF achieved by this method is only slightly higher than the FF obtained with the nontruncated Newtonian templates. One more time the Newtonian family of templates has failed to work as a ''good'' family of search templates; therefore, other post-Newtonian templates should be more seriously considered as possible candidates for search templates and be studied in detail. Even so, Schutz's idea might prove helpful for whatever post-Newtonian templates one chooses, and deserves further investigation.

IV. THE METHOD OF CONSTRUCTING A FAMILY OF SEARCH TEMPLATES

Sathyaprakash and Dhurandhar [5] have presented an algorithm for constructing a lattice of search templates that is capable of detecting any signal, of a certain minimal signal-to-noise ratio, that comes from a binary, the parameters of which lay within some range. However, their analysis is restricted to Newtonian signals and Newtonian templates, and to detectors with white noise. According to previous discussions their results do not reflect a realistic situation, and therefore, it should be reexamined. First, we will describe their algorithm and their result and then we will extend it to the more realistic case of a post^2-Newtonian signal and a post$^{1.5}$-Newtonian family of templates, and draw our conclusions. Their work will be translated here in the language of FF which, in our opinion, is simpler and has a more direct physical interpretation than the correlation function they had used.

The Newtonian waveforms depend on just three parameters t_C, ϕ_C, and $\mathcal{M}$ as one can verify by a quick look at Eqs. (3). The time of coalescence t_C can be handled directly at the stage of numerical cross correlation, and the phase at coalescence ϕ_C enters trivially in the waveform and only two values of it need to be considered [8]. Therefore, the problem of constructing a lattice of Newtonian templates to search for Newtonian signals transforms to the problem of filling the interval of chirp masses that correspond to potentially detectable signals, with a discrete set of chirp masses, so that for any signal represented by some fixed chirp mass within that interval there will be at least one member of the set of chirp masses that its corresponding Newtonian waveform produces a FF (by maximizing the relevant quantity over Δt_C, the only then free parameter to adjust) above, say, 0.9. The procedure to construct such a discrete set of chirp masses is the following: One starts with some arbitrary Newtonian template with a fixed chirp mass $\mathcal{M}_n$ (see Fig. 2) within the interval of interest and computes the dependence of FF on $\Delta(\mathcal{M}^{-5/3})$ by maximizing the quantity appearing on the right-hand side of Eq. (4) over Δt_C, then the only free parameter. Notice that now the roles of the signal and the
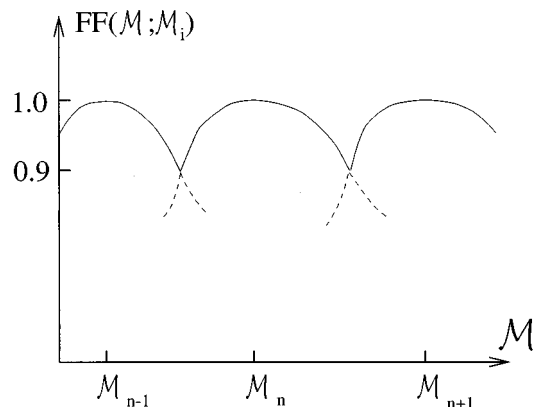

FIG. 2. The method used by Sathyaprakash and Dhurandhar [7] to estimate the number of Newtonian templates needed to detect a Newtonian signal with maximum accepted signal-to-noise reduction equal to 0.9: One keeps the chirp mass $\mathcal{M}_i$ of a template fixed and varies the chirp mass $\mathcal{M}$ of the signal until the corresponding FF drops to 0.9. This determines the range of detectability for that specific template.
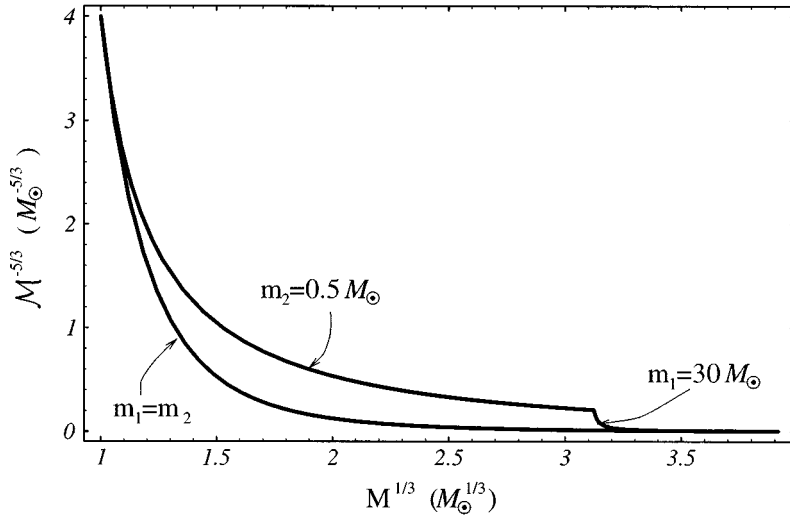
FIG. 3. This is the potentially detectable region of the parameter space, or in other words, the space of interest. Here we have assumed that the maximum possible mass included in the binary is $30M_\odot$ and the minimum one is $0.5M_\odot$. The bottom boundary corresponds to $m_1=m_2$; any point below this $m_1=m_2$ line corresponds to unphysical masses.

template are interchanged since the template is assumed fixed and one varies the parameters of the signal trying to achieve the best fitting. Although what we here call FF does not coincide with the initial definition of FF $[\Delta(\mathcal{M}^{-5/3})$ is assumed fixed, the maximization has been taken over the signal parameter $t_C]$ we will insist on calling this so, in order not to cause any confusion by introducing many new quantities that all measure the same thing: the best possible matching between template waveforms and signal waveforms in various cases. In every case the assumptions we make will be clearly exposed.

The range of chirp masses around $\mathcal{M}_n$ that produces FF's above 0.9 is the *range of detectability* for this template. When FF drops below the 0.9 level then one should find another template, characterized by $\mathcal{M}_{n-1}$ or $\mathcal{M}_{n+1}$, that produces FF's above 0.9 for chirp masses outside the range of detectability of the first template. Proceeding this way, one could cover the whole set of signal waveforms, that are in principle detectable, with a discrete set of templates that produce FF$\geqslant$0.9 for any Newtonian signal coming from a binary with chirp mass within that range.

Sathyaprakash and Dhurandhar found that for Newtonian signals from binaries with masses within the range $[0.5M_\odot,30M_\odot]$ one needs as many as 2450 Newtonian templates for detectors with white noise and lower frequency assumed 100 Hz. (The number includes the factor of 2, which arises from the two independent values we need for the phase at coalescence for every value of $\mathcal{M}^{-5/3}$.) Cross correlating a given data stream with such a number of templates in real time is well within the present computers' capabilities. But this optimistic message should be revised after considering the more realistic waveforms that are now available, and a more realistic detector noise.

Extending that method of constructing template families to post-Newtonian signals and templates is far more complicated since the corresponding waveforms no longer depend on only one parameter (aside from t_C and ϕ_C). The parameter space that one has to fill with carefully spaced templates is now two dimensional (if one considers template waveforms with no spin terms as we do). There was some hope after Sathyaprakash's work [11] that the effective dimensionality of the parameter space is still one. He showed, by using

post[1]-Newtonian templates and signals that there is some evidence of strong correlation between the chirp mass parameter and the post[1]-Newtonian parameter term; that is, by cleverly choosing some combination of these two parameters, one could reformulate the problem to a one-dimensional problem like the Newtonian one, with the chirp mass being replaced by this new parameter. Unfortunately, that was due to the assumption of white noise and the integration limits that were used; see [15]. Also, the irregularity of the parameter space, that was ignored in [11], turns out to be a serious issue as we shall see later.

In this paper we will assume that the spectral density of noise is given in Eq. (2b), the signals are described by the post[2]-Newtonian waveforms given in Eqs. (3) either with maximal β and σ terms [after substituting $S_1=m_1^2,S_2=m_2^2,\hat{S}_1=\hat{S}_2=\hat{L}$ in Eqs. (3e, 3f) one gets $\beta_{\max}=(113/12)-(19/3)(m_1m_2/M^2)$ and $\sigma_{\max}=(79/8)(m_1m_2/M^2)]$ or with vanishing spin terms, and the templates are described by post[1.5]-Newtonian waveforms with $\beta=0$ since they seem to be superior among all other two-parameter templates (see Table I).

The steps one should follow to construct a discrete family of post[1.5]-Newtonian templates to be used as search templates are the following. (1) One has to choose the two-dimensional parameter space to place his or her templates and signals on and then define its boundaries. We have chosen to use a power of the chirp mass, namely $\mathcal{M}^{-5/3}$, and a power of the total mass of the binary, namely $M^{1/3}$, as our two parameters and draw the boundaries in such a way that all masses in the interval $[0.5M_\odot,30M_\odot]$ are included. Our choice for the mass parameters makes it easy to rewrite the post-Newtonian terms in terms of them and in parallel it enables us to transform easily any combination of masses to the corresponding pair of the two mass parameters and vice versa. The price one has to pay then is an irregular region in the parameter space for all binaries under consideration (cf. Fig. 3), that we shall call *space of interest*. (2) One should find for each single signal point — practically, for several signal points — which lies in this space of interest, some template among the continuously parametrized chosen family of templates that produces the highest possible FF value.
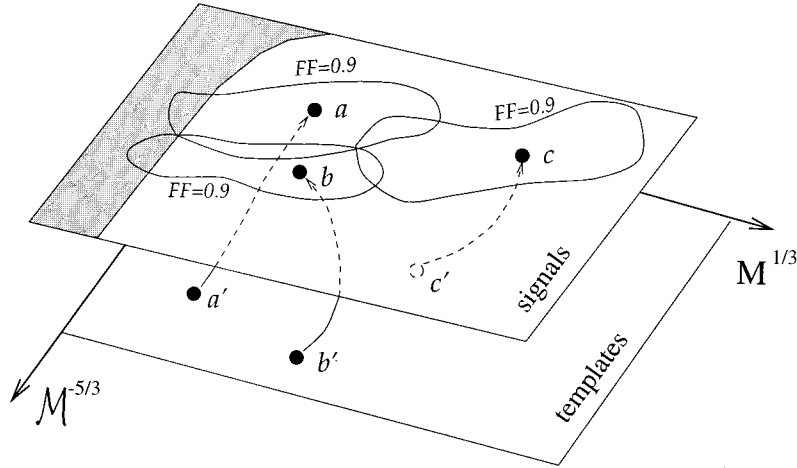
FIG. 4. The extension of Sathyaprakash-Dhurandhar method [5] to post-Newtonian signals and templates. The parameter space, where templates lie, is no more one-dimensional. Post-Newtonian templates depend not only on $\mathcal{M}^{-5/3}$ but on other functions of the masses as well. Therefore, instead of a series of bumps as in Fig. 2, one has now a large number of iso-FF contours covering completely the whole space of interest. If signals and templates are of different post-Newtonian order and/or post-Newtonian spin terms are included in the signals but not in the templates, then each signal-template pair that is producing the maximum FF among all other nearby signals (i.e., $a-a'$), corresponds to different mass parameters for the signal and the template; and the maximum FF value, then, is not unity but somewhat lower, since the matching can not be perfect. The grey region corresponds to signals that are not expected to be detectable; that is, signals lying outside the space of interest.

One does not have the luxury to do that by identifying the corresponding template with the signal since these two waveforms no longer have the same post-Newtonian form. Then one should explore how FF changes as one varies the signal's mass parameters, but keep the template fixed; here the quantity on the right-hand side of Eq. (4), from which FF is determined, has to get maximized over only Δt_C, as with the Newtonian case of [5]. Thus, one constructs contours of constant FF around each signal point; we shall call them *iso-FF contours* (see [16]). The space inside a 0.9-iso-FF contour is analogous to the region of detectability we defined earlier in this section for the one-dimensional case; in other words, it represents all signals for which the corresponding fixed template reduces the signal-to-noise ratio at most by 10%. (3) Finally, the space of interest should be completely covered with such 0.9-iso-FF contours, but they should be distributed as sparsely as possible so as to keep the number of templates low.

Now, counting the number of templates that are needed is not as easy as it was for the one-dimensional case. One can no longer estimate this number by dividing the area of the space of interest by the area of a 0.9-iso-FF contour because (1) some of the contours extend out of the boundaries of the space of interest, (2) a significant part of the contours' area is shared by two or more neighboring contours, due to their irregular shapes, and (3) the contours' sizes and shapes are not fixed but vary greatly with location (for a pictorial demonstration of all these counting problems see Fig. 4). Taking all these intricacies into account, we have attempted to give a rough estimate of the number of templates one would need to cover the whole space of interest with these 0.9-iso-FF contours.

More specifically, we have chosen several points in the space of interest, which correspond to some hypothetical sig-

nals, and computed the FF for each one assuming continuously varying parameters of the post$^{1.5}$-Newtonian template family. After fixing these best-matching templates we computed the FF output around the central signal point. We drew the corresponding 0.9-iso-FF contours and studied their shape and size. It should be noted that the template used to produce each 0.9-iso-FF contour does not necessarily lie within the boundaries of the contour since the waveforms used for the templates are quite different from the waveforms used for the signals; cf. Fig. 4.

In Fig. 5 we have plotted the shapes and sizes of some of these 0.9-iso-FF's for various locations in the space of interest. For each 0.9-iso-FF there exists a unique template waveform that produces FF$\geq$0.9 for all signals inside this 0.9-iso-FF contour. As these few contour plots indicate, the 0.9-iso-FF are in general very thin along the $\mathcal{M}^{-5/3}$ parameter with an average size of $\sim 2\times10^{-4}M_{\odot}^{-5/3}$, and quite elongated along the $M^{1/3}$ parameter. This was to be expected since the total mass parameter appears only in the post-Newtonian terms of a waveform; therefore, in order to change FF as much as tiny shifts in the chirp mass parameter do, a much larger shift in the total mass parameter is required. The actual horizontal size of the 0.9-iso-FF does not depend greatly on the horizontal position of the template (the $M^{1/3}$ value of the central signal), but it depends greatly on the value of the spin terms β and σ assumed for the post^2-Newtonian waveforms of the signals. For vanishing spins ($\beta=\sigma=0$) the corresponding 0.9-iso-FF contours are narrower (along $M^{1/3}$) than the ones with maximal spin terms (β,σ: maximal). This seemingly paradoxical effect is due to the opposite signs between the spin terms and the rest post$^{1.5}$- and post^2-Newtonian terms, that are not related to spin, respectively. When β and σ terms are maximal they
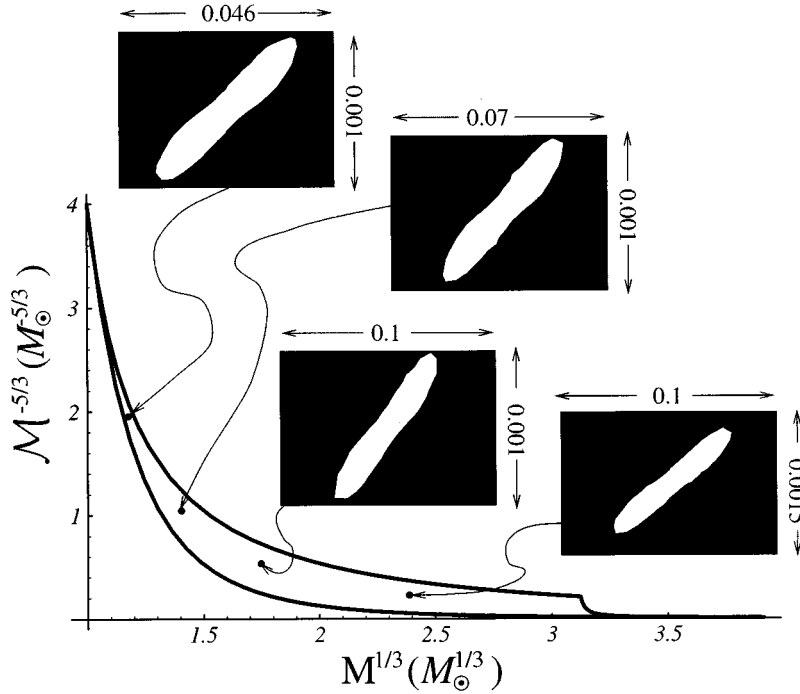
FIG. 5. This is again a plot of the parameter space showing the 0.9-iso-FF contours around several points residing inside the space of interest. Here, the templates are assumed to be of post$^{1.5}$-Newtonian order with $\beta=0$, while the signals are of post^2-Newtonian order with $\beta=0$, $\sigma=0$. The iso-FF contours have quite different sizes along the $M^{1/3}$ axis but not much different sizes along the $\mathcal{M}^{-5/3}$ axis. The method we have used to plot these contour plots is described in detail in Sec. IV.

reduce the magnitude of both these post-Newtonian terms, and thus they help post$^{1.5}$-Newtonian templates imitate the corresponding signal. In Fig. 6 we have plotted the number of contours that fit along the width (along $M^{1/3}$) of the space of interest, versus the chirp mass parameter, $\mathcal{M}^{-5/3}$. As one can see, much fewer templates are needed in the case of maximum spins that are aligned with the orbital angular mo-

mentum, than in the case of vanishing spins. From that plot one can deduce the average number of contours, thereby the average number of templates, that should be placed next to each other to fill the space of interest along its width. We found that number to be approximately 4.8 for the nonspinning binary case and 1.5 for the maximally spinning binary case. Now, by multiplying that number by the number of contours needed to cover the whole range of the chirp mass parameter we obtain the total number of templates one should use to pick up any signal with no more than 10% reduction in its signal-to-noise ratio. Finally, the total number of templates has been augmented by 20% (see [17]) to take into account the overlap between adjacent contours, and by a factor of 2 because of the two independent values of ϕ_C that need to be considered for each one of the templates we mentioned right above. Our results are presented in Table II.

The number of templates needed for a different space of interest is also shown in Table II. Namely, for binaries, the masses of which lie within the interval $[1M_\odot,30M_\odot]$. Part of the counting process that was described above had to be repeated once again for this case, since all three difficulties in connection with counting templates make it impossible to scale the number of templates with the limiting masses of the space of interest. However, the fact that the 0.9-iso-FF are so thin vertically suggests the following rough scaling law:

$$F \propto k((\mathcal{M}^{-5/3})_{\max}-(\mathcal{M}^{-5/3})_{\min}) \simeq k(\mathcal{M}^{-5/3})_{\max} \propto k m_{\min}^{-5/3},$$
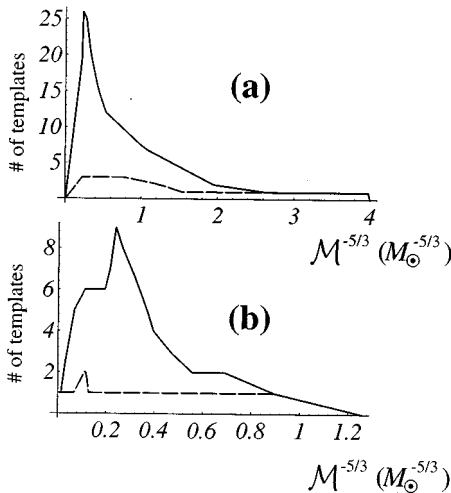(7)

FIG. 6. These diagrams show a crude estimation of the number of contours needed to fill up the parameter space along its width (along $M^{1/3}$) as a function of $\mathcal{M}^{-5/3}$. The solid lines correspond to post^2-Newtonian signals with vanishing spin terms ($\beta=\sigma=0$), while the dashed lines correspond to post^2-Newtonian signals with maximal spin terms (β,σ: maximal). The templates we have used are assumed to be of post$^{1.5}$-Newtonian order with $\beta=0$, as everywhere in our analysis. (a) For the case of $m_{\min}=0.5M_\odot$, (b) for $m_{\min}=1.0M_\odot$. These plots have been used to compute the total number of templates, quoted in Table II.

where the proportionality factor k, which denotes the average number of contours along the horizontal direction, is not a constant but depends on the limiting masses in a much softer way though; cf. Fig. 6. The maximum mass limit is not very crucial in determining the number of templates, which, on the other hand, cannot be extremely high since then the

TABLE II. This table presents the total number of post[1.5]-Newtonian templates with $\beta=0$ that a template family should contain in order to produce a FF≥ 0.9 for any post[2]-Newtonian signal from a binary with any combination of masses within the interval $[0.5M_\odot, 30M_\odot]$ or within the interval $[1\ M_\odot, 30M_\odot]$. Signals with vanishing or maximal spin parameters are assumed. Any spin-induced precessional effects have been neglected since the spins — whenever they are present — have been considered to be aligned with respect to the binary's orbital angular momentum. The numbers of templates have been computed by using the method described in Sec. IV. Also, we are showing the computing power that each case demands. The numbers, quoted here, for the computing power have been based on Eq. (9) assuming $f_u = 300$ Hz.

	Range of masses in $M_\odot$	No. of templates	Gflops
P^2-N signal:	[0.5,30]	231 000	12.2
($\beta=\sigma=0$)	[1,30]	42 000	2.1
P^2-N signal:	[0.5,30]	73 000	3.9
(β,σ maximal)	[1,30]	13 300	0.7

frequency corresponding to the last stable orbit would be so low that only a few cycles of the signal would enter the LIGO-VIRGO band.

V. COMPUTING POWER

In the actual data process one has to transform the real data from the time domain to the frequency domain, take the product between the data and all preconstructed templates — after having weighted the latter by $f^{7/3}/S_n(f)$ — and finally transform these products back to the time domain (see Fig. 7). This whole process requires, for F templates,

$$\mathcal{N}_{\text{flop}} \simeq 3n(\log_2 N + 2F + F\log_2 n) \simeq 3nF(2+\log_2 n), \quad (8)$$

where N is the number of elements the data stretch consists of, and n is the number of elements kept in the frequency domain [since very high frequencies of the signal are highly suppressed by the weighting function $f^{-7/3}/S_n(f)$, only a narrow range of frequencies should be used]. Obviously $n = N(2f_u/f_s)$, where f_s is the sampling rate of the data and f_u is the uppermost frequency kept in the frequency domain.

Now, there should be some overlap between successive real data stretches in order to avoid problems arising from circular correlation; see [10]. Let us call this overlapping fraction x. This overlap xN should be as long as the longest expected signal. If one wants to keep up with the incoming data, the number of floating operations quoted in Eq. (8) should be performed in a time period $T = N(1-x)/f_s$. Thus the computing power one needs is related to the number of templates through

$$\mathcal{R} \simeq \frac{1.8}{1-x}\left(\ln_2 \frac{2f_u\tau_{\max}}{x} + 2\right)\left(\frac{F}{10^6}\right)\left(\frac{f_u}{300\text{Hz}}\right)\text{Gflops}, \quad (9)$$

where $\tau_{\max}$ is the time duration of the longest template in the template family. One, then, has to compute the optimal value for x and replace it in Eq. (9) in order to find the required computing power. The optimal value for x is of the order of 0.05 for $f_u = 300$ Hz and $\tau_{\max} \simeq 5.5 \times 10^3$ sec (this is the time a binary with $m_1 = m_2 = 0.5M_\odot$ needs to sweep upwards in frequency from 10 Hz to f_u). (One should note that the op-
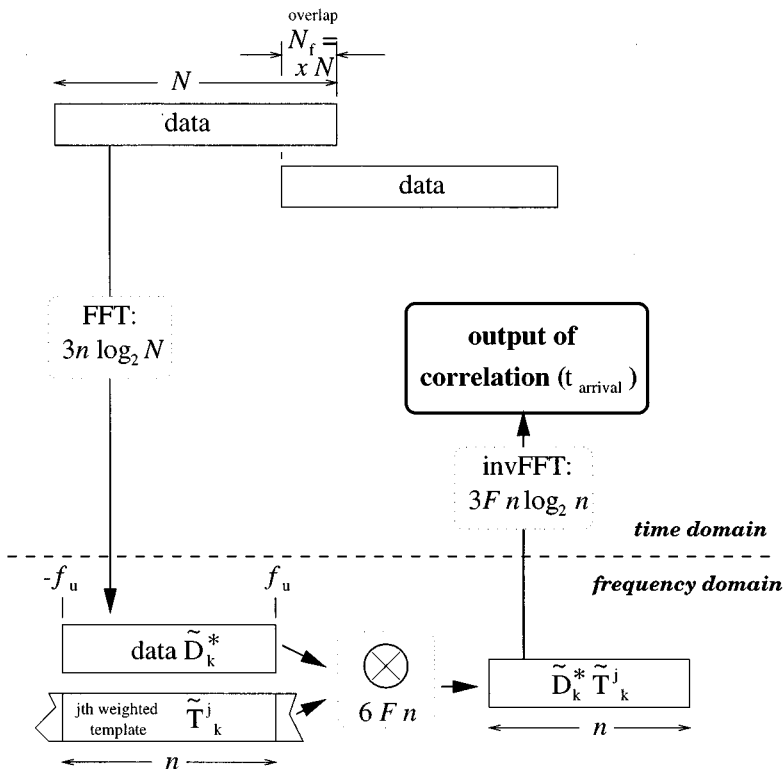

FIG. 7. This is a schematic diagram presenting the whole data analysis process at the stage of detection. First, a data stretch consisting of N real numbers gets fast Fourier transformed. But since all frequencies above ~ 300 Hz are mainly coming from noise, the corresponding data could be disregarded. That reduces the amount of floating operations from $3N\log_2 N$ to $3n\log_2 N$, where n is the number of data kept in the frequency domain. Then, these n complex numbers should be multiplied with all, say, F, preconstructed weighted templates. That means $6Fn$ floating point operations. Finally, these products should be fast Fourier transformed to obtain the correlation for each template. This final process demands $3Fn\log_2 n$ floating operations.

timal value of x does not depend crucially on the assumed values of f_u and $\tau_{\max}$.) The computing power quoted in Table II is based on Eq. (9) with assumed value for f_u, 300 Hz. These numbers are remarkably close to the numbers obtained by Owen [18] by a somewhat different method.

VI. SPIN-INDUCED PRECESSIONAL EFFECTS INCLUDED

Up to this point we have assumed that even if spins are nonvanishing they are aligned with the binary's orbital angular momentum to make sure that no precession of the orbital plane occurs, and thus, the gravitational signal waveforms are simply described by the post-Newtonian waveforms that are given in Eqs. (3). Now, if we consider arbitrary angles between spins and orbital angular momentum the signal's parameter space becomes much richer and the two-dimensional post$^{1.5}$-Newtonian template family used in Sec. IV can hardly mimic *in some cases* the true precessionally modulated signal and produce high FF values. The larger the misalignment angles the more difficult it is to find a post$^{1.5}$-Newtonian template (with $\beta = 0$) that adequately mimics the true signal (cf. Ref. [9]). Also other parameters of the binary affect the complexity of the signal and accordingly the adequacy of such post$^{1.5}$-Newtonian templates. Apart from the geometry of the binary what is actually directly responsible for the deep modulation of the signal waveform is the opening angle λ_L for the precession of $\hat{\mathbf{L}}$ (the unit vector along the orbital angular momentum of the binary) and not the spin-orbital angular momentum angle $\hat{\mathbf{S}}\hat{\mathbf{L}}$, which was used in Ref. [9] as the main parameter connected with spins, to demonstrate the degradation of the effectiveness of various template families as the precessional effects get more and more pronounced. The opening angle λ_L is given by

$$\cos\lambda_L = \frac{1 + \gamma\cos\phi}{\sqrt{1 + \gamma^2 + 2\gamma\cos\phi}}, \qquad (10)$$

where $\gamma = S/L$ depends on the masses involved and the instantaneous frequency, $\cos\phi = \hat{\mathbf{L}} \cdot \hat{\mathbf{S}}$, and $S, \hat{\mathbf{S}}$ are the magnitude of the total spin $|\mathbf{S}_1 + \mathbf{S}_2|$ and the unit vector along the total spin $(\mathbf{S}_1 + \mathbf{S}_2)/|\mathbf{S}_1 + \mathbf{S}_2|$, respectively. In the following we will assume that both spins have magnitude $S_i = M_i^2$ and they always remain parallel to each other ($\hat{\mathbf{S}}_1 = \hat{\mathbf{S}}_2$); essentially one then has to take into account a single spin vector. These assumptions make the situation more dramatic by maximizing the spin-induced precessional effects and on the other hand they simplify our analysis since the precessional motion for the case of one spin (simple precession) is known analytically (see Ref. [12]), and can be easily implemented in our computer code for calculating FF. (The assumption that $\mathbf{S}_1 \| \mathbf{S}_2$ is actually wrong, since each spin traces a different precession path and the angle between the two spins changes continuously, but the precessional behavior one gets under this assumption still resembles quite well the true precession, as was shown in [12].)

The larger the opening angle λ_L, the larger the portion of the geometries defining the orientation and location of the binary with respect to the detector, which lead to low FF values because of deep amplitude modulation and mainly

because of deep phase modulation of the waves. Of course the plain post$^{1.5}$-Newtonian template family is not "flexible" enough to mimic this complicated modulated signal waveforms. If signals from binaries with considerable opening angles — which carry quite a lot of information and could ultimately serve as excellent tests of general relativity — are not to be missed, then more complicated templates should be used. This would magnify the computational task. How much is the issue addressed in the following analysis.

Since most of the signal-to-noise ratio is picked up at a frequency lower than the frequency at which the detectors are more sensitive (see Fig. 2 of Ref. [2]), more specifically, at ~ 50 Hz for the advanced LIGO detectors, we have chosen to use the opening angle value at 50 Hz (henceforth denoted $\lambda_L^{(50)}$) as the main parameter to measure the intensity of the precessional effects. In Fig. 8 we are showing a density plot of $\lambda_L^{(50)}$ in grey scale (black represents lowest angle) covering the whole space of interest for some fixed ϕ angle. At least for ϕ angles up to 90°, $\lambda_L^{(50)}$ is a monotonically increasing function of ϕ, therefore the pattern showing up in this density plot is more or less independent of ϕ; only the maximum value of $\lambda_L^{(50)}$ depends on ϕ. One can see clearly that the region of the space of interest that might cause the greatest problems with respect to spin-induced precessional effects is the upper right corner of it; that is, the region of the binaries with the highest mass ratios. That means that the 0.9-iso-FF contours (analyzed in Sec. IV for nonmodulated signals), when drawn around these regions of potentially deep-modulated signals, are expected to contain a very low percentage of realistic modulated signals for which the corresponding fixed post$^{1.5}$-Newtonian template produces FF values above 0.9.

To get a feeling for the fraction of extremely spinning binaries for which the post$^{1.5}$-Newtonian template family proves adequate (producing FF values above 0.9) we have compiled in Fig. 9 a large amount of information concerning the distribution of FF for various $\lambda_L^{(50)}$ angles as one varies the geometry of the binary with respect to the detector's arms. We have picked up a few points inside one of the 0.9-iso-FF contours for nonmodulated post^2-Newtonian signals with maximal β and σ terms, and *approximately* estimated the percentage of binary geometries that are producing FF≥ 0.9 for any possible $\lambda_L^{(50)}$. This estimation was based on the following approximate relation (for a proof see Appendix A):

$$\mathrm{FF}(\mathcal{Q}, \lambda_L^{(50)}; \mathrm{geometry}) \simeq \mathrm{FF}(\mathcal{Q}, \lambda_L^{(50)}; \mathrm{no\ precession})$$
$$\times \mathrm{FF}(\mathcal{Q}_*, \lambda_L^{(50)}; \mathrm{geometry}) \ , \tag{11}$$

where $\mathcal{Q}_*$ and $\mathcal{Q}$ are the "central point" — the one producing the highest FF if precession is absent — and an arbitrary point inside the 0.9-iso-FF contour, respectively. This relation simply states that one can separate the drop of signal-to-noise ratio due to spin-induced precession alone [rightmost term in Eq. (11)] from the one due to nonoptimal combination of parameters of the nonmodulated signal and the template [left term on the right-hand side of Eq. (11)]. The term "geometry" denotes some arbitrary fixed geo-
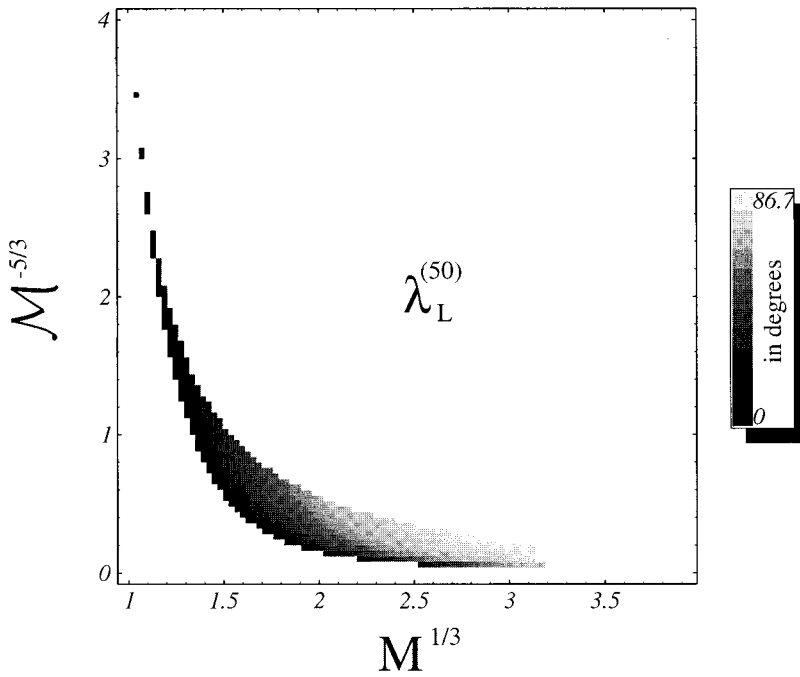
FIG. 8. This density plot diagram shows which regions of the parameter space are most affected by spin-induced precession effects (lighter regions). What has been actually plotted here in grey scale, is the $\lambda_L^{(50)}$ value for all possible combinations of masses within $[0.5M_\odot, 30M_\odot]$. The misalignment angle between orbital angular momentum and spins has been assumed here to be 90°, but since $\lambda_L^{(50)}$ is a monotonic function of $\hat{\mathbf{L}}\mathbf{S}$, at least for $\hat{\mathbf{L}}\mathbf{S} \leqslant 90°$, this diagram gives a more or less correct distribution of $\lambda_L^{(50)}$ for any moderate misalignment angle; however the maximum $\lambda_L^{(50)}$ angle depends on $\hat{\mathbf{L}}\mathbf{S}$. (The dotted form of the upper part of the diagram is only due to the number of points that were chosen to be depicted.)

metrical configuration of the binary and the detector. The term FF($\mathcal{Q}, \lambda_L^{(50)}$; no precession) has no reference to geometry since the output of FF is independent of the binary-detector geometry when there is no precession. When computing this FF though, one should use for the post-Newtonian phase terms of the signal, the same β and σ terms that are assumed for the other two FF terms *with* precession.

One can see clearly in Fig. 9 that for $\lambda_L^{(50)} \gtrsim 25°$ FF is above 0.9 only for 50% of the binaries at the central point,

and even for $\lambda_L^{(50)} < 25°$ the contours that contain at least *some* binaries, for which the fixed post $^{1.5}$-Newtonian template produces FF$\geqslant 0.9$, shrink considerably (e.g., for $\lambda_L^{(50)} = 25°$ there is almost no binary producing FF$\geqslant 0.9$ outside the 0.925-iso-FF contour). The consequence of this is twofold: (1) One has to increase the number of templates and reduce their spacing in order to have some chances to detect a signal from a moderately precessing binary. This increase depends on the maximum $\lambda_L^{(50)}$ value one considers realistic and insists on searching for such a binary. (2) For $\lambda_L^{(50)}$
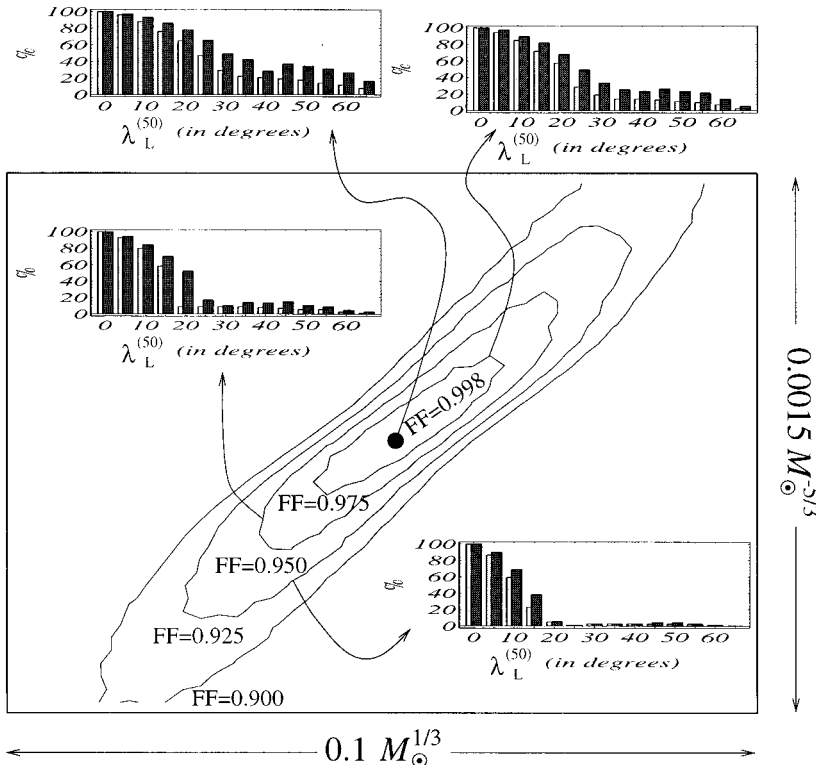

FIG. 9. By compiling the values of the FF for all possible geometrical configurations, and using Eq. (11) for several $\lambda_L^{(50)}$, we obtained the percentages of precessing binaries with masses around the masses of the central point $(10M_\odot, 1.4M_\odot)$ and opening angle $\lambda_L^{(50)}$ that produce a FF above 0.9. (The central point of the diagram represents the $\mathcal{Q}_*$ point of our discussion in Appendix A while any other point around could be thought of as the $\mathcal{Q}$ point of our analysis.) The grey histograms show the percentages when we use the simple post $^{1.5}$-Newtonian templates with those fixed $\mathcal{M}^{-5/3}$ and $M^{1/3}$ values that produce the highest possible FF value (0.998) for the central point's signal when precession is not present. The black histograms arise when the more complicated family of templates that allow for an oscillating term in their phase are used; see Eq. (12). The contours shown at the main diagram are the iso-FF contours discussed in Sec. IV that refer to signals from nonprecessing binaries; here, they serve as the multiplicative factor FF($\mathcal{Q}, \lambda_L^{(50)}$; no precession) of Eq. (11).

above 50°, no matter how densely one fills the space of interest with post$^{1.5}$-Newtonian templates, they are practically inadequate to detect such precessing binaries.

Possible improvement could offer a more advanced family of templates that might be able to mimic the spin-induced modulation of the waves. Having chosen properly the parameters of the post$^{1.5}$-Newtonian template, one obtains a total phase in the expression from which one computes FF [$\Delta\psi(f)$ plus the phase evolution which is hidden in the PM term; see Eq. (4)] that looks like an oscillatory phase, due to precession, superimposed on an almost constant, throughout the most sensitive frequency band of the detector, phase; even the secular evolution of the precessionally modulated phase, that might arise in some special geometric configurations (cf. [9]), could disappear by properly adjusting the template's parameters. Therefore, the simplest extension of the post$^{1.5}$-Newtonian template family one could think of is a family of post$^{1.5}$-Newtonian templates with an additional oscillatory phase. More specifically, since the precession angle $\alpha(f)$ (see [9,12]) evolves $\propto f^{-2/3}$ or f^{-1}, depending on the relative sizes of L and S, a good choice for the frequency dependence of the additional oscillatory phase would be either $f^{-2/3}$ or f^{-1}. We have chosen the one that is $\propto f^{-2/3}$ since only if S is of about the same order as L the precessional effects are noticeable. The templates that we have chosen to use have the same form as the post$^{1.5}$-Newtonian templates given in Eqs. (3), with an extra oscillatory term added on its phase $\psi_{1.5}^{(\beta=0)}(f)$:

$$\psi_{1.5}^{\text{new}}(f) = \psi_{1.5}^{(\beta=0)}(f) + \mathcal{C}\cos(\delta + \mathcal{B}f^{-2/3}). \tag{12}$$

The precise frequency dependence does not seem to be crucial since only a small number of precession cycles occur within the sensitive range of the detector; we have verified this by testing the behavior of both $f^{-2/3}$ and f^{-1} frequency terms in the additional phase.

These new templates introduce three new parameters $\mathcal{C}, \delta, \mathcal{B}$, besides the old ones $\Delta t_C, \Delta\phi_C, \Delta(\mathcal{M}^{-5/3}), \Delta(M^{1/3})$, thus raising substantially the total number of templates. On the other hand they greatly improve the FF values. The code we have used to compute the FF's does not perform a simultaneous maximization of the quantity appearing in Eq. (4) over all six parameters [maximization over one of them, ϕ_C, has already been achieved by replacing the quantity to be maximized with its absolute value; cf. Eq. (4)]. Rather it computes the maximum over the old parameters first and then over the new ones; this is justified by the nearly independent contribution of these two sets of parameters on FF (see Appendix B). In Fig. 9 the FF values obtained (black histograms) when these new templates are used are compared with the old FF values (grey histograms), for various $\lambda_L^{(50)}$ values.

Unfortunately the inclusion of three more parameters in the templates' waveforms will skyrocket the number of templates since each old template will then split in roughly 10^6 new templates (see Appendix B). That leads to a completely unrealistic total number of templates with respect to computing power — at least for the next coming decade or so. Nevertheless, it offers a conceivable way to expand the detectability of our templates to become able to search for such

precessing binaries in the future. These new templates could also be used at a more detailed afterdetection stage for extracting all possible spin information and thus improving the extraction of other parameters that are nonrelated to spin [2].

VII. CONCLUSIONS

This paper addresses the question of the number of templates needed for detection as well as the form the templates should have and the method to construct them from the outset, assuming, for first time, a more or less realistic signal waveform from a coalescing binary (post^2-Newtonian) and a realistic noisy detector (the advanced LIGO one). By using FF (the fitting factor introduced in [9]) not as a measure of adequateness of a template family but as a tool to set the spacing between neighboring templates, we obtained a number of templates almost two orders of magnitude higher than the number estimated in Ref. [5] which was based on Newtonian signals, Newtonian templates, and detectors with white noise.

Our analysis suggests that neither the Newtonian family of templates nor any other family of templates with as few parameters as the Newtonian one is adequate for detection purposes. At least one more mass parameter is necessary for the candidate family of templates. This has been verified independently by Owen [18] for the restricted case of post^1-Newtonian signals and templates.

Finally, we have analyzed the role of spins in the number of templates. If one ignores the spin-induced precession of the binary then the spin terms in the higher post-Newtonian order terms have a moderate impact on the total number of parameters. However, if one allows for precession effects then not only the number of templates has to raise considerably but even then a great number of signals might remain undetectable due to inadequate matching between the simple templates and the highly precessionally modulated signal. Essential improvement might offer more complicated templates, like the ones introduced in Eq. (12), but then the price is a formidable number of templates, well beyond the capabilities of the near-future computers. These new complicated templates could be used after detection to improve the signal-to-noise ratio and offer some information about the spins, which then could be used to extract more accurately other astrophysical parameters like the masses [2].

This work is a first step in expanding the post-Newtonian templates so as to include ''corrections'' that mimic the true precessionally modulated gravitational waves. Further investigation has to be done to enable this rich structure, due to precession, be revealed.

APPENDIX A: DECOMPOSITION OF FF INTO A NONOSCILLATING-PHASE PART AND AN OSCILLATING-PHASE PART

Consider the following version of FF:

$$\mathrm{FF}(\mathcal{Q},\lambda_L^{(50)};\mathrm{geometry}) = \max_{\Delta t_C} \frac{\left| \int_0^\infty df[f^{-7/3}/S_n(f)]e^{i\Delta\psi(f)}\mathrm{AM}\times\mathrm{PM} \right|}{\sqrt{\left[\int_0^\infty df[f^{-7/3}/S_n(f)] \right]\left[\int_0^\infty df[f^{-7/3}/S_n(f)](\mathrm{AM})^2 \right]}}. \tag{A1}$$

The only thing that makes this expression different from the usual formula for FF [cf. Eq. (4)] is that the quantity on the right-hand side is maximized over only one parameter, Δt_C. Equation (A1) gives the FF value for a family of post$^{1.5}$-Newtonian templates located at a fixed location $\mathcal{Q}_*$ on the $[\mathcal{M}^{-5/3}, M^{1/3}]$ space — thus, having only t_C as a free parameter to adjust — and a post^2-Newtonian signal, located at position $\mathcal{Q}$ on the $[\mathcal{M}^{-5/3}, M^{1/3}]$ space, coming from a precessing binary with a specific geometry relative to the detector's arms and a fixed opening angle at 50 Hz, $\lambda_L^{(50)}$.

Now, assume that all secular evolution of PM has been transferred into $\Delta\psi(f)$ term, and thus, PM is just a purely oscillating phase term. After the maximization over Δt_C, $\Delta\psi(f)$ acquires a $\cup$-like shape (or a $\cap$-like one as in Fig. 10) with its flat part centered around 50 Hz. The reason is that $f^{-7/3}/S_n(f)$ is maximum at about 50 Hz (for the advanced LIGO detector), thus the phase term should be kept nearly constant near that frequency. The larger the distance between $\mathcal{Q}$ and $\mathcal{Q}_*$, the narrower the opening of $\cup$ (or $\cap$), since only at $\mathcal{Q}_*$ the differences between the template's mass parameters and signal's mass parameters are optimal, and, therefore, $\Delta\psi(f)$ has the widest possible flat bottom (or top).

One, then, could approximate $\Delta\psi(f)$ as

$$\Delta\psi(f) = \begin{cases} \mathrm{const} & \text{for } f_l \leq f \leq f_u, \\ \infty & \text{for } f < f_l < 50\ \mathrm{Hz}, \\ \infty & \text{for } f > f_u > 50\ \mathrm{Hz}, \end{cases} \tag{A2}$$

where f_l and f_u are two frequencies on either side of 50 Hz, that depend on the location of $\mathcal{Q}$; more specifically, the smaller the distance between $\mathcal{Q}$ and $\mathcal{Q}_*$ the larger the interval $f_u - f_l$. Hence Eq. (13) simplifies to

$$\mathrm{FF}(\mathcal{Q},\lambda_L^{(50)};\mathrm{geometry}) \simeq \frac{\left| \int_{f_l(\mathcal{Q})}^{f_u(\mathcal{Q})} df[f^{-7/3}/S_n(f)]\mathrm{AM}\times\mathrm{PM} \right|}{\sqrt{\left[\int_0^\infty df[f^{-7/3}/S_n(f)] \right]\left[\int_0^\infty df[f^{-7/3}/S_n(f)](\mathrm{AM})^2 \right]}}. \tag{A3}$$
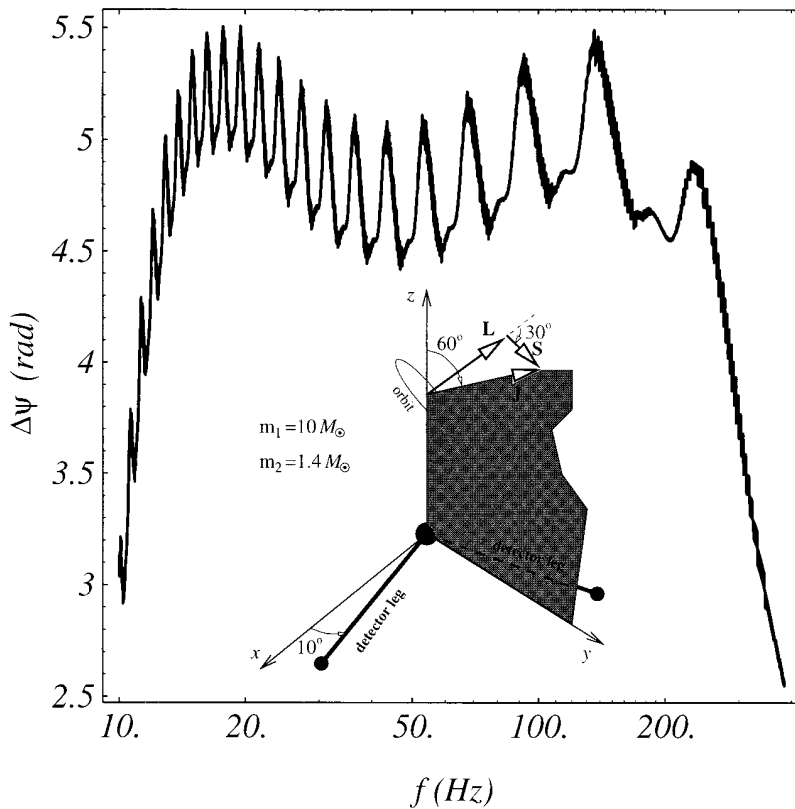

FIG. 10. This plot shows how the phase difference between a post^2-Newtonian signal from a precessing binary (shown in the schematic picture at the bottom of the diagram) and the best-matching simple post$^{1.5}$-Newtonian template depends on frequency. One can see clearly its wavy $\cap$ shape that we discussed in Appendix A. This picture justifies the addition of an extra oscillatory term on the phase of our post$^{1.5}$-Newtonian templates; cf. Eq. (12).

Now, since the modulation terms PM and AM are oscillating rather fast compared to the rate that $f^{-7/3}/S_n(f)$ evolves, one could replace their effect with a constant suppression factor, and rewrite Eq. (A3) as the following:

$$\text{FF}(\mathcal{Q},\lambda_L^{(50)};\text{geometry}) \simeq \frac{\left| \int_{f_l(\mathcal{Q})}^{f_u(\mathcal{Q})} df[f^{-7/3}/S_n(f)] \times (\text{supr. factor}) \right|}{\sqrt{\left[\int_0^\infty df[f^{-7/3}/S_n(f)] \right]\left[\int_0^\infty df[f^{-7/3}/S_n(f)](\text{AM})^2 \right]}}$$

$$= \frac{\int_{f_l(\mathcal{Q})}^{f_u(\mathcal{Q})} df[f^{-7/3}/S_n(f)]}{\int_{f_l(\mathcal{Q}_*)}^{f_u(\mathcal{Q}_*)} df[f^{-7/3}/S_n(f)]} \frac{\left| \int_{f_l(\mathcal{Q}_*)}^{f_u(\mathcal{Q}_*)} df[f^{-7/3}/S_n(f)] \times (\text{supr. factor}) \right|}{\sqrt{\left[\int_0^\infty df[f^{-7/3}/S_n(f)] \right]\left[\int_0^\infty df[f^{-7/3}/S_n(f)](\text{AM})^2 \right]}}. \qquad (A4)$$

Remember that $\mathcal{Q}_*$ is the location of that special signal that our one-parameter family of templates would match very well if precessional modulation was not present. Therefore, $\int_{f_l(\mathcal{Q}_*)}^{f_u(\mathcal{Q}_*)} df f^{-7/3}/S_n(f)$ could be replaced by $\int_0^\infty df f^{-7/3}/S_n(f)$. That brings Eq. (A4) to the form

$$\text{FF}(\mathcal{Q},\lambda_L^{(50)};\text{geometry}) \simeq \frac{\int_{f_l(\mathcal{Q})}^{f_u(\mathcal{Q})} df[f^{-7/3}/S_n(f)]}{\int_0^\infty df[f^{-7/3}/S_n(f)]} \frac{\left| \int_{f_l(\mathcal{Q}_*)}^{f_u(\mathcal{Q}_*)} df[f^{-7/3}/S_n(f)]\text{AM}\times\text{PM} \right|}{\sqrt{\left[\int_0^\infty df[f^{-7/3}/S_n(f)] \right]\left[\int_0^\infty df[f^{-7/3}/S_n(f)](\text{AM})^2 \right]}}, \qquad (A5)$$

which is just the same with Eq. (11), apart from small differences that arise from approximating $\Delta\psi(f)$ by a constant within the interval $[f_l,f_u]$ and ∞ outside this interval.

In the following, we will give an example that demonstrates the accuracy of Eq. (11). For a post²-Newtonian signal coming from a binary with $m_1 = 10M_\odot$, $m_2 = 1.4M_\odot$, and $\mathbf{LS} = 30^\circ$, which is located at the position shown in Fig. 10, the best matching post¹·⁵-Newtonian template is the one whose parameters are differing from the signal's parameters by $\Delta t_c = -3.1$ msec, $\Delta(\mathcal{M}^{-5/3}) = 9.002 \times 10^{-4} M_\odot^{-5/3}$, $\Delta(M^{1/3}) = 0.7945 M_\odot^{1/3}$. The FF produced then is $\text{FF}(\mathcal{Q}_*,\lambda_L^{(50)};\text{geometry}) = 0.9490$. On the other hand, if one uses templates with the same $\mathcal{M}^{-5/3}, M^{1/3}$ as before to match another signal nearby $\mathcal{Q}_*$, say $\mathcal{Q}$ with masses $m_1 = 10.255\,20M_\odot$, $m_2 = 1.374\,26M_\odot$, and with the same $\lambda_L^{(50)}$ as for $\mathcal{Q}_*$ the computed FF values are $\text{FF}(\mathcal{Q},\lambda_L^{(50)};\text{geometry}) = 0.8884$, if the binary is precessing with the same $\lambda_L^{(50)}$ as before, and $\text{FF}(\mathcal{Q},\lambda_L^{(50)};\text{no precession}) = 0.9218$, if the binary is not precessing, respectively. The approximate equation (11) is accurate to the level of 1.5%.

APPENDIX B: TEMPLATES WITH AN EXTRA OSCILLATORY TERM IN THEIR PHASE

During the orbital inspiral of a binary, if at least one of the bodies is rapidly rotating, then the general relativistic spin-orbit and spin-spin coupling cause the binary's orbital plane to precess. This precession leads to a modulation of gravitational waves both in amplitude and in phase. As was shown in [9] the phase modulation has more dramatic consequences than the amplitude modulation. Here, we are focusing our interest on trying to improve the matching between a signal from a precessing binary and a post¹·⁵-Newtonian family of templates by adding in the templates' phase an extra term that resembles the true modulated phase of a signal. The modulated phase could happen to grow secularly, but that could in general get fixed quite well by properly adjusting the templates parameters. What remains then, is a complicated oscillation in phase that evolves at the same rate as the precession itself; cf. Fig. 10. Therefore, a natural extra term we could add to the templates' phase is a simple sinusoidal term that has the same frequency dependence as precession. Of course, the actual oscillatory phase term of a real signal is much more complicated than a simplistic sinusoidal term, as one can see from Fig. 10. Nevertheless, a sinusoidal term, like the one given in Eq. (12), with the appropriate triad of amplitude ($\mathcal{C}$), initial phase (δ), and ''wave number'' ($\mathcal{B}$), can greatly enhance the matching ability of a template.

In order to get a feeling of the necessary spacing between templates in the $[\mathcal{C},\delta,\mathcal{B}]$ parameter space we have explored the drop of correlation between simple sinusoidal phase terms as a function of parameter mismatching. More specifically, we have computed numerically the function
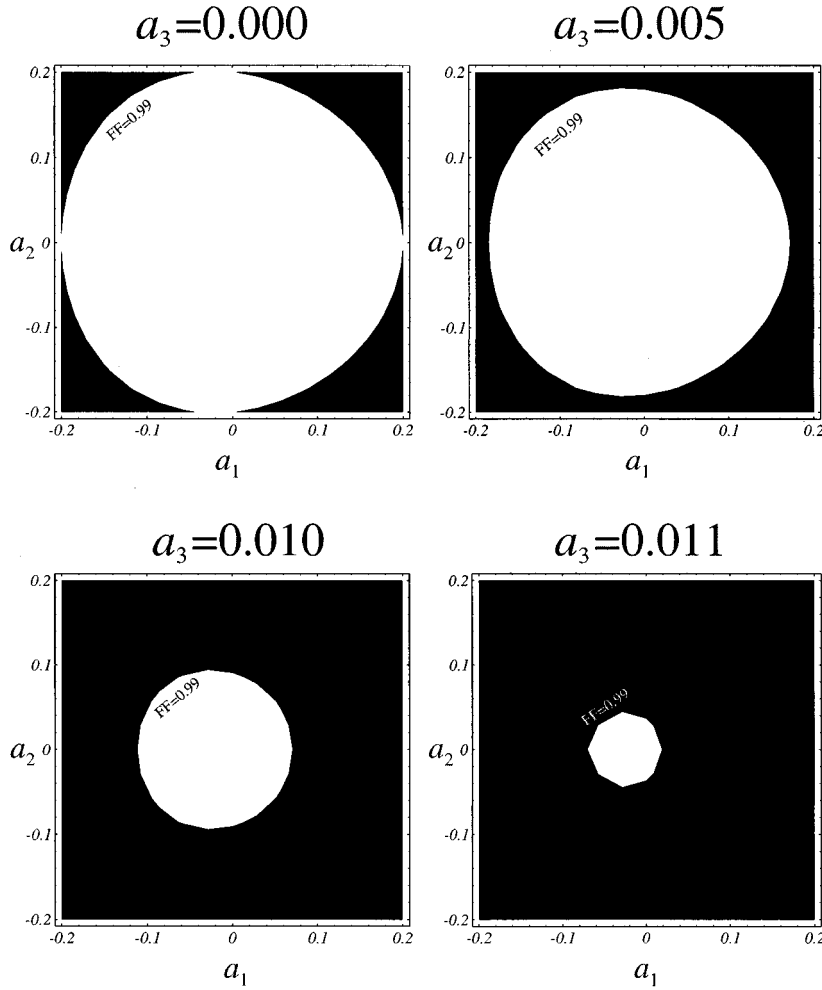
FIG. 11. Here we have plotted the contours $c(a_1,a_2,a_3)=0.990$ at various a_3 values, where $c(a_1,a_2,a_3)$ models the correlation between the new expanded templates and the signal from a precessing binary; see Eq. (B1). The sizes of the contours indicate that in order to cover the whole $[a_1,a_2,a_3]$ parameter space with as few templates as possible one should choose templates spaced by roughly $[0.1,0.1,0.005]$, respectively.

$$c(a_1,a_2,a_3)=\frac{\left| \int_{-10\pi}^{10\pi} dx \ \exp(i\{\cos(x)-(1+a_1)\cos[a_2+(1+a_3)x]\}) \right|}{20\pi}. \tag{B1}$$

Apart from an amplitude term this function has the form of FF before the maximization over the three new parameters of the oscillatory term has been carried out. Here, the signal is assumed to have a simple sinusoidal phase given by $\psi^{\text{signal}}(x)=\cos(x)$, while the template is assumed to have a similar phase form with slightly different amplitude, initial phase, and wave number. The integration over ten cycles is justified from the fact that ten is roughly the number of precessions occur in the range of frequencies over which the advanced LIGO detectors have high sensitivity. From Fig. 11 it is clear that in order to achieve sufficiently good phase matching [producing $c(a_1,a_2,a_3)\geqslant 0.99$] one should choose templates spaced by roughly $[0.1,0.1,0.005]$ in the $[a_1,a_2,a_3]$ parameter space.

Now, going back to the somewhat different phase term $\mathcal{C}\cos(\delta+\mathcal{B}/f^{2/3})$, that was introduced in Eq. (12) as an improvement of the post$^{1.5}$-Newtonian templates, these numbers could be interpreted as follows: (i) The values of $\mathcal{C}$ should be spaced by about 0.1; that means that we need

about 30 values of $\mathcal{C}$ to cover all possible amplitudes up to π. (ii) The values of δ should be spaced by about 0.1; that means that we need about 60 values of δ to cover all possible phase displacements up to 2π. (iii) Since our example suggests that nearby values of $\mathcal{B}$ should differ by no more than 0.5%, the number of $\mathcal{B}$ one would then need is $\simeq \ln(\mathcal{B}_{\min}/\mathcal{B}_{\max})/\ln 0.995$. The minimum and maximum value of $\mathcal{B}$, $\mathcal{B}_{\min}$, and $\mathcal{B}_{\max}$, respectively, depend on the range of masses, spin magnitudes, and misalignment angles between spin and orbital angular momentum. After exploring the values of $f^{2/3}[\alpha(f)-\alpha(f=\infty)]$, where $\alpha(f)$ is the precession angle, for the most extreme parameter values we have inferred that the ratio $\mathcal{B}_{\min}/\mathcal{B}_{\max}$ is of the order of 1:20; therefore one should use $\simeq 600$ individual values of $\mathcal{B}$. Hence, every single old template should be split to $30\times 60\times 600\times 2\simeq 2\times 10^6$ new templates to make it possible to improve the correlation between templates and a true signal from a precessing binary. The factor 2 comes from the fact that for large opening angles λ_L, the orbital precession

could be such that the modulated phase oscillates with twice the frequency of precession; see [9].

One should also keep in mind that there are two or more, depending on the magnitude of λ_L, regions in the space of the binary-detector geometry that are characterized by differ- ent secular evolution of the modulated phase. For each of these regions, one needs a different combination of $\Delta t_C, \Delta(\mathcal{M}^{-5/3}), \Delta(M^{1/3})$ parameters to cancel out these secularly or nonsecularly evolving phases. That raises the total number of templates to a formidable $\sim 10^{11}$–10^{12}.

---

[1] C. Cutler, T. A. Apostolatos, L. Bildsten, L. S. Finn, E. E. Flanagan, D. Kennefick, D. M. Markovic, A. Ori, E. Poisson, G. J. Sussman, and K. S. Thorne, Phys. Rev. Lett. **70**, 2984 (1993).

[2] C. Cutler and E. Flanagan, Phys. Rev. D **49**, 2658 (1994).

[3] T. A. Apostolatos, D. Kennefick, A. Ori, and E. Poisson, Phys. Rev. D **47**, 5376 (1993).

[4] C. Cutler, D. Kennefick, and E. Poisson, Phys. Rev. D **50**, 3816 (1994).

[5] B. S. Sathyaprakash and S. V. Dhurhandhar, Phys. Rev. D **44**, 3819 (1991).

[6] A. Kròlak, K. Kokkotas, and G. Schäfer, Phys. Rev. D **52**, 2089 (1995).

[7] S. V. Dhurhandhar and B. S. Sathyaprakash, Phys. Rev. D **49**, 1707 (1994).

[8] B. F. Schutz, in *The Detection of Gravitational Waves*, edited by D. G. Blair (Cambridge University Press, Cambridge, England, 1991), pp. 406–452.

[9] T. A. Apostolatos, Phys. Rev. D **52**, 605 (1995).

[10] B. F. Schutz (private communication).

[11] B. S. Sathyaprakash, Phys. Rev. D **50**, 7111 (1995).

[12] T. A. Apostolatos, C. Cutler, G. J. Sussman, and K. S. Thorne, Phys. Rev. D **49**, 6274 (1994).

[13] A. Abramovici, W. E. Althouse, R. W. Drever, Y. Gürsel, S. Kawamura, F. J. Raab, D. Shoemaker, L. Siewers, R. E. Spero, K. S. Thorne, R. E. Vogt, R. Weiss, S. E. Whitcomb, and M. E. Zucker, Science **256**, 325 (1992).

[14] L. Blanchet, T. Damour, B. R. Iyer, C. M. Will, and A. G. Wiseman, Phys. Rev. Lett. **74**, 3515 (1995).

[15] It is obvious that by using the noise spectrum of the advanced LIGO detector, the importance of high frequencies ($f>200$ Hz) will be strongly suppressed and on the other hand many more cycles than in the case of [11] will be included at the process of phase matching and signals due to the low seismic cutoff frequency ($\simeq 10$ Hz). The latter is in fact the main cause of disagreement between our work and that of Ref. [11], since in our case we are trying to achieve phase matching between templates and signals over many more cycles.

[16] For sufficiently low FF values an iso-FF contour could in prin- ciple be disconnected, consisting of more than one ''islands.'' Particularly, for the case of 0.9-iso-FF contours we have not observed any formation of such islands.

[17] It can be shown that in order to cover a long, thin strip with dimensions $L \times d$ ($L \gg d$) with circles of radius R ($2R>d$) one will need $(1+o)(L/2R)$ circles, where o is a factor that arises because of the overlap of adjacent circles. This overlap factor has an average value of 0.24 for $0 \leq d \leq 4R/\sqrt{5}$ ($4R/\sqrt{5}$ is the critical width of the strip, above which more than one column of circles should be used to cover the strip in a more economic way). The overlap factor grows a bit higher when wider strips are taken into account, but since the space of interest (cf. Fig. 3) is quite thin along the horizontal direction for a long vertical interval, the overlap factor of 20% we have assumed is a rea- sonable estimate.

[18] B. J. Owen, Phys. Rev. D **53**, 6749 (1996).